ELSEVIER

Chemosphere 58 (2005) 1071–1078

CHEMOSPHERE

www.elsevier.com/locate/chemosphere

Photocatalytic oxidation of gaseous DMF using thin film TiO_2 photocatalyst

Chiu-Ping Chang [a,b], Jong-Nan Chen [a], Ming-Chun Lu [c,*], He-Yuan Yang [a]

[a] *Institute of Environmental Engineering, National Chiao Tung University, Hsinchu 300, Taiwan*
[b] *Department of Environmental Engineering and Health, Yuanpei Institute of Science and Technology, 306 Yuanpei Street, Hsinchu 300, Taiwan*
[c] *Department of Environmental Resources Management, Chia Nan University of Pharmacy and Science, Tainan 717, Taiwan*

Received 11 November 2003; received in revised form 8 September 2004; accepted 15 September 2004

Abstract

The heterogeneous photocatalytic oxidation of gaseous *N*,*N*′-dimethylformamide (DMF) widely used in the manufacture of synthetic leather and synthetic textile was investigated. The experiments were carried out in a plug flow annular photoreactor coated with Degussa P-25 TiO_2. The oxidation rate was dependent on DMF concentration, reaction temperature, water vapor, and oxygen content. Photocatalytic deactivation was observed in these reactions. The Levenspiel deactivation kinetic model was used to describe the decay of catalyst activity. Fourier transform infrared (FTIR) was used to characterize the surface and the deactivation mechanism of the photocatalyst. Results revealed that carbonylic acids, aldehydes, amines, carbonate and nitrate were adsorbed on the TiO_2 surface during the photocatalytic reaction. The ions, NH_4^+ and NO_3^-, causing the deactivation of catalysts were detected on the TiO_2 surface. Several treatment processes were applied to find a suitable procedure for the regeneration of catalytic activity. Among these procedures, the best one was found to be the H_2O_2/UV process.

Keywords: Photocatalysis; Titanium dioxide; *N*,*N*′-dimethylformamide; Deactivation; Regeneration

1. Introduction

The interest in heterogeneous photocatalysis to remove trace organic compounds present in air exhaust streams and in indoor environments is intense and increasing. This is a process in which the illumination of an oxide semiconductor, usually the anatase form of titanium dioxide, creating photoexcited electrons (e^-) and holes (h^+). The attractive advantages of this technology are: (i) photocatalytic oxidation can proceed at ambient temperature and pressure; (ii) the excitation source can be sunlight or low-cost fluorescent light sources; (iii) photocatalysts are generally nontoxic, inexpensive, and chemically and physically stable; and (iv) final oxidation products are usually innocuous (Xu and Raftery, 2001; Zhao and Yang, 2003).

In gas-phase, the reaction intermediates and reaction products tend to accumulate on the catalyst surface causing the deactivation of the catalyst. This phenomenon has already been elegantly described in

* Corresponding author. Tel.: +886 6 2660489; fax: +886 6 2663411.
E-mail addresses: mmclu@mail.chna.edu.tw, mclu@ms17.hinet.net (M.-C. Lu).

0045-6535/$ - see front matter © 2004 Elsevier Ltd. All rights reserved.
doi:10.1016/j.chemosphere.2004.09.072

other previous works (Peral and Ollis, 1997; Huang et al., 1999; Alberici et al., 2001; Sun et al., 2003). Peral and Ollis (1992) detected some catalyst deactivation during photocatalytic oxidation of 1-butanol. Sauer and Ollis (1996) proposed the photocatalyst deactivation happening in single-pass fixed-bed photoreactors for cumulative contaminant conversions. Peral and Ollis (1997) studied the oxidation of gas-phase organics containing three different heteroatoms (Si, N, and S), and observed the irreversible catalyst deactivation in the case of decamethyltetrasiloxane, pyrrole and indole. Huang et al. (1999) presented that carboxylic acid species, –N–N=O species, and some other carbonaceous species accumulated on the catalyst surface during photooxidation of triethylamine. Alberici et al. (2001) studied the photocatalytic oxidation of pyridine, propylamine and diethylamine, and observed that the inorganic species (such as ammonium and nitrate) produced in the photocatalytic reaction induced the loss of catalyst activity. Piera et al. (2002) reported the deactivation of TiO_2 during the photocatalytic oxidation of gaseous ethanol, and used several surface treatment processes to recover catalytic activity. Sun et al. (2003) investigated the photocatalyzed decomposition of gas-phase octamethyltrisiloxane. They found the catalyst was deactivated by the formation and accumulation of hydroxylated SiO_x on catalyst surface. Thus, detailed studies of the characterization of surface chemical species and deactivation pathway are desired.

N,*N*′-dimethylformamide (DMF) is commonly used in the chemical industry as a solvent, especially for the factory producing synthetic leather and synthetic textile. There was 40 000 tones/year of gaseous DMF emission from the polyurethane synthetic leather factories in Taiwan. Conventional wet washing method cannot remove this contaminant completely. The DMF of effluent gas usually causes strong odor (Lin et al., 1999). For human, the organ of main toxic action is the liver. In several studies, testicular germ-cell tumours were identified among workers who had been exposed to DMF (Ducatman et al., 1986; CDCP, 1989). Therefore, DMF was classified in group 2B (possibly carcinogenic to humans) by International Agency for Research on Cancer (IARC) of the World Health Organization (WHO, 1989). The allowable exposure concentration is 10 ppm, recommended by the Council of Labor Affairs in Taiwan.

The present work was to explore the photocatalytic oxidation of DMF in gas-phase. Effects of DMF concentrations, water vapor, reaction temperature and content of oxygen on the oxidation rate were examined. Catalyst deactivation and regeneration were investigated with most of this work being devoted to the characterization of chemical species of the catalyst surface.

2. Experimental

2.1. Catalyst and chemicals

The catalyst used in this study was Degussa P-25 titanium dioxide with a primary particle diameter of 30 nm. The TiO_2 powder contains both anatase and rutile phases. The surface area of powder is $50 \pm 15\ m^2\ g^{-1}$ (BET). The TiO_2 thin film catalyst was prepared using a spread coating method. It was coated on the outer surface of inner tube using a well mixed slurry of 10 wt% TiO_2 in deionized water. The TiO_2-coated tube was heated at 110 °C for 1.5 h. Two areas of TiO_2 were used in our study, 110 and 170 cm^2. A TiO_2 loading density of 0.09 mg cm^{-2} was obtained by weighting the tube before and after the coating.

Other chemicals were purchased from the Merck Company: sodium nitrate (99.5%), ammonium chloride (99.8%), ammonium nitrate (99.5%), *N*,*N*′-dimethylformamide (99.8%), hydrogen peroxide (35%) and potassium bromide (spectroscopy).

2.2. Equipment

The photocatalytic degradation processes were carried out in a continuous reactor, depicted schematically in Fig. 1. The annular reactor was fabricated from the Pyrex glass. It was of 30 mm inside and 37 mm outside diameter with 300 mm long. The total volume of reactor was 110 cm^3. Illumination was provided by a 10-W black light lamp (Sankyo Denki Japan-BLB) with a maximum light intensity output at 365 nm. DMF and water were drawn by syringes to stainless steel tube and wrapped with heating tape for vaporization. The temperature of heating tape was controlled at 140 °C. The concentrations of DMF and water were controlled by the syringe pumps (KD Scientific, Model 250). The mass flow controller (Brooks, 5850E) controlled the flow rates of nitrogen and oxygen. The reactor was also wrapped with heating tape to maintain the temperature of reaction. Behind the reactor, the dewpoint sensor (SHAW, green spot sensor) was equipped to measure the humidity of outlet flow.

2.3. Analysis

The DMF concentrations were analyzed by a China GC-9800F gas chromatograph equipped with a flame ionization detector (FID) and a Cobalwax packed column (2 m long × 3.2 mm o.d.). Nitrogen was used as the carrier gas. The temperatures of oven and detector were kept at 130 °C and 200 °C, respectively. Carbon dioxide from DMF mineralization was analyzed with an FID and a porapak N column (2 m long × 3.2 mm o.d.) after converting CO_2 to CH_4 through a Rh-catalyst methanizer. For the purpose of methanizer,

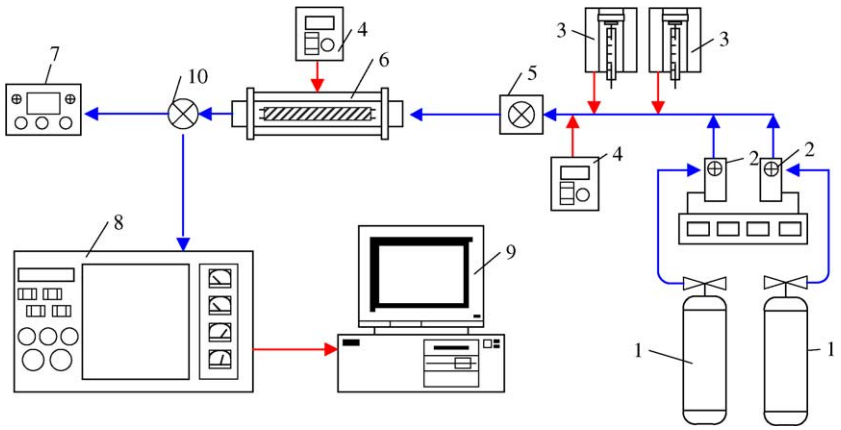

Fig. 1. Setup of experimental apparatus: (1) gas cylinder (N_2 and O_2); (2) mass flow controller; (3) syringe pump; (4) heater; (5) mixer; (6) photocatalytic reactor; (7) dewpoint sensor; (8) GC/FID; (9) computer; (10) sampling valve.

hydrogen was used as the carrier gas. The temperatures of porapak N column and methanizer were kept at 130 °C and 300 °C, respectively.

The used catalyst after the photocatalytic oxidation of DMF was washed with 25 ml deionized water. The solution was shaken for 1 h by the ultrasonic shaker and filtered with 0.45 μm membrane. The filtrate was analyzed by an ion chromatograph (IC, Dionex Model 120) using IonPac AS12A column for cation analysis and IonPac CS12 column for anion analysis. After the photooxidation experiments, the catalysts were mixed with potassium bromide, the weight ratio of KBr/TiO_2 was 100/1. The mixed powder was pressed to form KBr pellet, and then the adsorbed species on the surface of TiO_2 could be analyzed by an FTIR instrument (Bomem DA8.3).

2.4. Catalyst regeneration

Seven regeneration processes were expressed as follows:

1. Dry Air (DA): Catalyst was exposed to continuous flow of air (20% oxygen and 80% nitrogen) at 100 °C for 1 h.
2. Dry Air/UV (DA/UV): Catalyst under UV irradiation was exposed to continuous flow of air at 100 °C for 1 h.
3. O_2/UV: Catalyst was exposed to 1 h continuous flow of 100% O_2 at 100 °C under UV irradiation.
4. Wet Air/UV (WA/UV): Catalyst was exposed with to a continuous air containing vaporized water (1160 μM) at 100 °C and UV irradiation for 1 h.
5. H_2O/UV: Ten ml of H_2O solution was directly sprayed on the TiO_2 surface. The catalyst was exposed to continuous flow of air at room temperature for 15 min and simultaneous UV irradiation. Then, the catalyst was dried at 100 °C.
6. H_2O_2/UV: Ten ml of H_2O_2 solution (1.06 M) was directly sprayed on the TiO_2 surface. The catalyst was exposed to continuous flow of air at room temperature and UV irradiation for 15 min. Then the catalyst was dried at 100 °C.
7. H_2O_2: Ten ml of H_2O_2 solution (1.06 M) was directly sprayed on the TiO_2 surface. The catalyst was dried at 100 °C. After regeneration, H_2O_2 was detected by titanium sulfate (Snell and Snell, 1949). There was no residual H_2O_2 on the TiO_2 surface.

3. Results and discussion

3.1. The kinetics of DMF photooxidation

Fig. 2 presents the photooxidation profiles for different concentrations of DMF on titanium dioxide thin films. The oxidation rate of DMF decreased with reaction time, indicating the deactivation of catalyst. The deactivation kinetic model proposed by Levenspiel (1999) has been widely used in the area of the kinetics of catalyst deactivation to calculate the loss of catalytic activity over reaction time. In general, the deactivation is dependent on the concentration of reactants. The decay reaction could be described as follow:

$$-\frac{da}{dt} = k_d C_D^n a^d \quad (1)$$

$$a = \frac{r_D}{r_{D0}} \quad (2)$$

where a is the activity of catalyst, k_d is rate constant for the deactivation of catalyst, C_D is the inlet concentration of DMF, n is the order of concentration, d is the order of

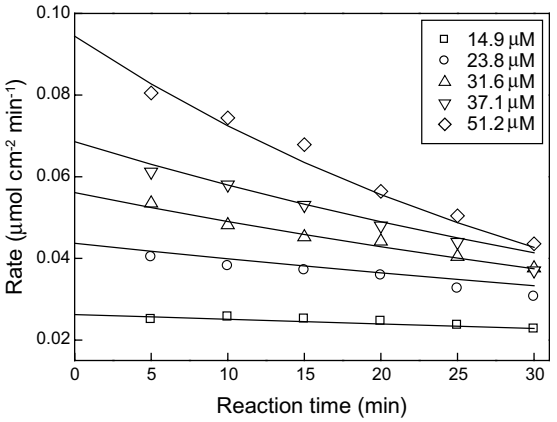

Fig. 2. Effect of DMF concentration on photocatalytic degradation. (Experimental condition: oxygen content = 20%; humidity = 3.25 μM; reaction temperature = 100 °C; area of catalyst film = 110 cm^2.)

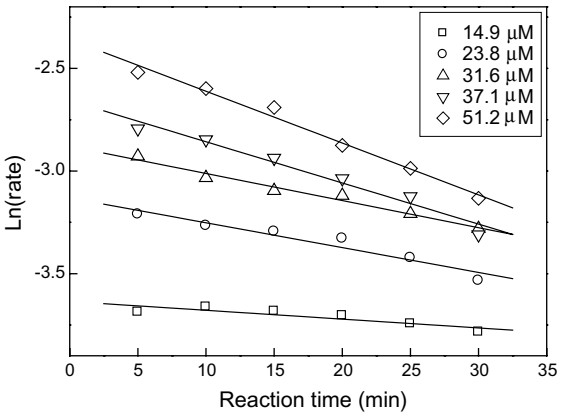

Fig. 3. Deactivation kinetics for DMF in photocatalytic degradation.

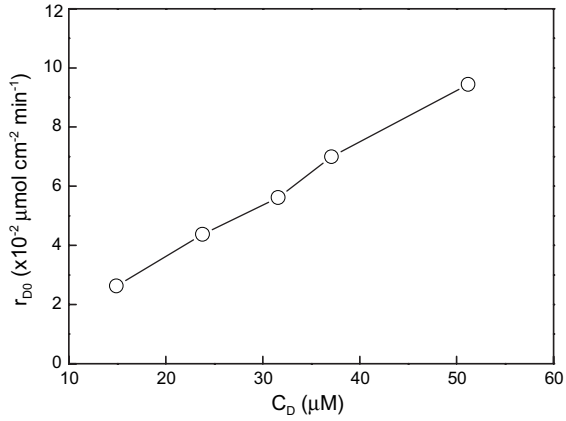

Fig. 4. The initial reaction rate for the photooxidation of DMF at different inlet concentration. (Experimental condition: oxygen content = 20%; humidity = 3.25 μM; reaction temperature = 100 °C; area of catalyst film = 110 cm^2.)

deactivation, r_D is the reaction rate of DMF, and r_{D0} is the initial reaction rate of DMF.

When used Eq. (1) to analyze experimental data, it is usually found that the deactivation order, d, is 1 (Niu and Hofmann, 1997; Monzón et al., 2003). Therefore, Eq. (1) can be simplified as follow:

$$-\frac{da}{dt} = k_d C_D^n a \tag{3}$$

The integration of Eq. (3) leads to the following expressions:

$$-\ln a = k_d C_D^n t \tag{4}$$

By substituting Eq. (2) in Eq. (4), the reaction rate as a function of time can be obtained as follow:

$$\ln r_D = \ln r_{D0} - k_d C_D^n t \tag{5}$$

The relationship between $\ln(r_D)$ and reaction time is linear, shown in Fig. 3. The slope and intercept are given by

$$\text{Intercept} = \ln r_{D0} \tag{6}$$

$$\text{Slope} = -k_d C_D^n \tag{7}$$

Fig. 4 presents that the initial reaction rate increased with increasing the inlet concentration of DMF. The rate of photocatalytic oxidation was controlled by adsorption of reactant and desorption of product. Increasing the concentration of DMF increased the adsorption of reactant on TiO_2 surface. Hence, the oxidation rate increased with increasing the concentration of DMF.

By plotting Eq. (7) in a linear form (ln(slope) versus $\ln(C_D)$), the parameters k_d and n can be found. From the slope and intercept of the regression line, the k_d and n have been estimated as 1.04×10^{-4} $\mu mol^{-1.4}$ min^{-1} and 1.4, respectively. Therefore, the deactivation kinetics can be described by the following model equation:

$$-\frac{da}{dt} = 1.04 \times 10^{-4} C_D^{1.4} a \tag{8}$$

By substituting the r_{D0}, C_D, n and k_d values into Eq. (5), the analytical relationship between r_D and t is obtained. The solid lines drawn in Fig. 2 represent this relationship; a good fitting of the model to the experimental data is observed.

3.2. Reaction temperature

In general, temperature is one of important factors in gas–solid heterogeneous photocatalytic reaction. Photo-

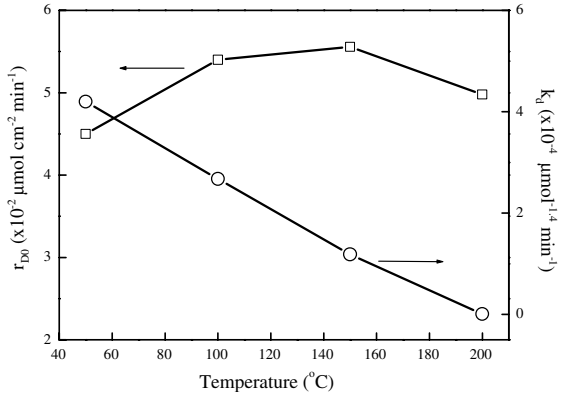

Fig. 5. The variation of r_{D0} and k_d under different reaction temperature. (Experimental condition: inlet DMF concentration = 31.2 μM; oxygen content = 20%; humidity = 3.25 μM; area of catalyst film = 110 cm^2.)

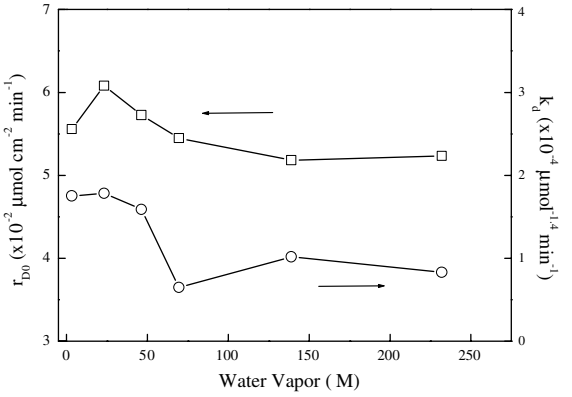

Fig. 6. The variation of r_{D0} and k_d under different water vapor. (Experimental condition: inlet DMF concentration = 32.5 μM; oxygen content = 20%; reaction temperature = 100 °C; area of catalyst film = 110 cm^2.)

catalytic degradation of trichloroethylene and methanol was more effective at a moderate temperature than at high temperatures (Kim et al., 2002). The yield of acetone from 2-propanol oxidation was maximized at a surface temperature of 77 °C and decreased to low values at −23 °C and 327 °C (Brinkley and Engel, 1998). In order to explore the effect of temperature, different temperatures ranging from 100 °C to 200 °C were applied in this study. The initial reaction rate of DMF increased with increasing the temperature ranging from 100 °C to 150 °C (Fig. 5). Above 150 °C, the rate was reduced with increasing temperature. The values of k_d decreased with increasing temperature. It displays that the deactivation of catalyst was serious at lower temperature.

3.3. Water vapor

Activation of TiO_2 can be achieved through the adsorption of a photon of ultraviolet ray ($\lambda < 365$ nm), which results in the promotion of an electron, e^-, from the valence band to conduction band, with the simultaneous generation of a hole, h^+, in the valance band (Eq. (9)). The holes may be trapped by adsorbed water to form hydroxyl radicals (Eq. (10)).

$$TiO_2 \xrightarrow{h_v(\lambda<365\ nm)} h^+_{vb} + e^-_{cb} \quad (9)$$

$$h^+_{vb} + H_2O_{ads} \rightarrow {}^{\bullet}OH_{ads} + H^+ \quad (10)$$

However, the influence of water vapor on the photooxidation is complex. Water plays an important role in the formation of the active species ($^{\bullet}$OH, Eq. (10)). Adsorbed water is an effective electron–hole recombination center leading to less photoactivity (Linsebigler et al., 1995). Therefore, adsorbed water could interfere the oxidation of organics. In order to examine the effect of water vapor, different amounts of water vapor were applied to a fixed concentration of DMF. Fig. 6 shows the r_{D0} and k_d versus water vapor concentration varying from 3.25 μM to 250 μM. The photocatalytic degradation rate was enhanced by water vapor with concentration up to 46 μM, and then inhibited above this concentration. The values of k_d decreased with increasing water vapor. During the oxidation process, the oxidation rate of DMF raised by the production of hydroxyl radical increased with increasing water vapor. However, water competed same adsorptive sites with DMF (Yamazaki et al., 1999). Hence, at high concentration of water vapor, it is beneficial to adsorption of water, leading to the inhibition of DMF oxidation.

3.4. Content of oxygen

Oxygen is an electron accepter. In UV/TiO_2 system, it can trap the electron to reduce the probability for recombination of electron/hole pairs (Eq. (11)).

$$O_{2(ads)} + e^- \rightarrow {}^{\bullet}O^-_{2(ads)} \quad (11)$$

The r_{D0} increased and k_d reduced with increasing the oxygen content from 0% to 20% when temperature was 100 °C, water vapor was 3.25 μM, and DMF was 31.4 μM (Fig. 7). Both of r_{D0} and k_d reached a stable level when the oxygen content was higher than 20%. Increasing the concentration of gaseous oxygen increased the amount of adsorbed O_2 on the TiO_2 surface. Gas-phase oxygen could reduce the probability for recombination of electron/hole pairs because it adsorbed on the surface to react with electrons forming super-oxide anion radicals ($^{\bullet}O_2^-$; Eq. (11)). In addition, super-oxide ions are highly reactive species that can oxidize DMF. Consequently, the more O_2 content can promote the photocatalytic oxidation of DMF. However, the amount of surface site adsorbed O_2 was constant. It caused that

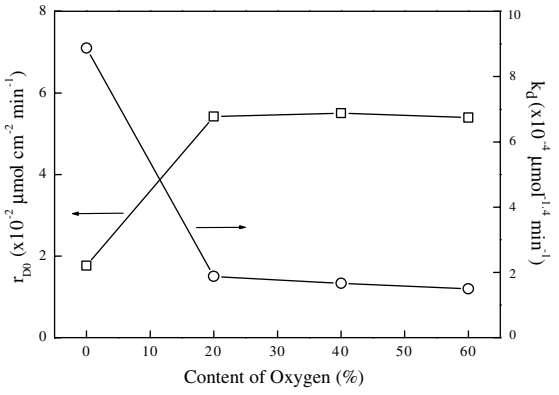

Fig. 7. The variation of r_{D0} and k_d under different oxygen content. (Experimental condition: inlet DMF concentration = 31.4 μM; humidity = 3.25 μM; reaction temperature = 100 °C; area of catalyst film = 110 cm^2.)

increasing the concentration of gaseous oxygen did not increase the reaction rate of DMF when O_2 content was more than 20%.

3.5. Intermediated and final products of DMF oxidation

The surfaces of the catalyst under different experimental conditions were analyzed using FTIR as shown in Fig. 8. The fresh catalyst presented an obvious sharp peak at 1646 cm^{-1}, which may be due to bending vibration of surface hydroxyl groups of TiO_2. Additionally, a broad band at 3440 cm^{-1}, which is attributed to an O–H stretching vibration, was observed on the fresh catalyst.

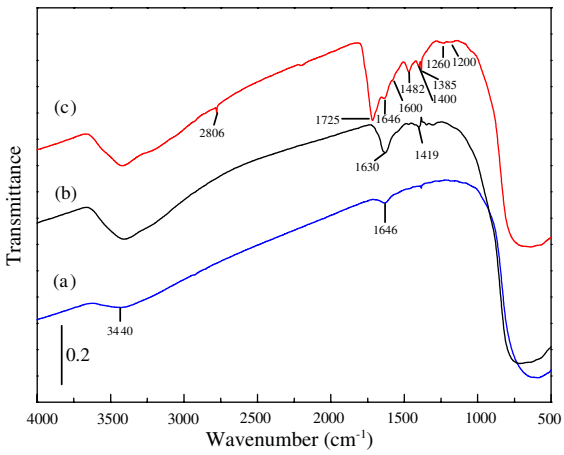

Fig. 8. FTIR spectra of catalysts (a) before exposed to DMF; (b) after saturated with DMF (c) after DMF oxidation 150 min. (Experimental condition: inlet DMF concentration = 26.0 μM; oxygen content = 20%; humidity = 3.25 μM; reaction temperature = 100 °C; area of catalyst film = 170 cm^2.)

After exposure of the fresh catalyst with DMF vapor, the spectrum of catalyst is shown in Fig. 8(b). There was new bands in 1630 cm^{-1} and 1419 cm^{-1}, which are assigned to C=O stretching vibration and aldehydic C–H bending vibration of DMF. After the catalyst was in equilibrium with the reactant, oxidation of DMF was carried out for 150 min. The spectrum of the reacted catalyst is shown in Fig. 8(c). Two peaks at 1630 cm^{-1} and 1419 cm^{-1} disappear, indicating that DMF was almost degraded. A distinct peak at 1725 cm^{-1} was observed, which is assigned to C=O stretching vibration of –COOH (carboxylic acid) or –COH (aldehydes). There is a peak at 2806 cm^{-1}, which was due to the C–H stretching vibration of the aldehydic hydrogen. At 1400 cm^{-1}, it may be due to the aldehydic C–H bending vibration. The C–O stretch of carboxylic acids was observed at 1260 cm^{-1}. At 1200 cm^{-1} and 1600 cm^{-1}, they are due to the C–N stretching vibration and the NH_2 scissoring vibration of primary amines. These reveal that the intermediates of DMF photooxidation may be formaldehyde, formic acid and methylamine. In addition, the N–O stretch of nitrate and C–O stretch of carbonate appear at 1385 cm^{-1} and 1482 cm^{-1}, respectively. They are the final products of DMF oxidation.

Klare et al. (2000) found the inorganic products including NH_3/NH_4^+, NO_2^- and NO_3^- in photooxidation of alkylamines. After degradation of nitrogen-containing organic compounds, NH_4^+ and NO_3^- were trapped at the TiO_2 surface (Alberici et al., 2001). After 1 h and 2 h of irradiation, the catalyst was scraped from the reactor and washed by diluted water. The washing solution was filtered and analyzed by an IC. The amount of ammonium (NH_4^+) and nitrate (NO_3^-) increased with increasing irradiated time. Nitrogen balances were close to 50%. Nitrite ions were not detected in these samples. It is possible that nitrite ions were rapidly oxidized to nitrate. During the period of illumination, the nitrogen-containing organic compound was initially transformed to ammonium, which was oxidized to nitrite and nitrate as shown in Eqs. (12) and (13) (Alberici et al., 2001).

$$2H_2O + NH_4^+ + 6h^+ \rightarrow NO_2^- + 8H^+ \quad (12)$$

$$H_2O + NO_2^- + 2h^+ \rightarrow NO_3^- + 2H^+ \quad (13)$$

The effect of deactivation for ammonium and nitrate ions was investigated. The catalyst surface was sprayed with the solution of ammonium chloride, sodium nitrate or ammonium nitrate and dried for 30 min at 80 °C. The conversion and mineralization of DMF followed the sequence: pure $TiO_2 \cong TiO_2 + NaNO_3 > TiO_2 + NH_4Cl \cong TiO_2 + NH_4NO_3$. Obviously, the ammonium ions on catalyst surface would deactivate the catalyst. On the contrary, the influence of nitrate ions on the catalytic activity was small. The deactivation of TiO_2 by ammonium ions was due to the consumption of h^+

was consumed by ammonium (Eq. (12)). Nitrate, the highest oxidative type of nitrogen, did not capture the h^+ to reduce catalyst activity.

3.6. Regeneration of catalyst

Seven regeneration processes of TiO_2 activity were studied in order to find the suitable procedure for the regeneration of catalytic activity. Every regeneration process used in this study followed the steps: (1) the fresh catalyst was used to carry out the first photocatalytic run and regenerated afterwards; (2) the second photocatalytic run was carried out, then the catalyst was regenerated again; (3) the third photocatalytic run and regeneration were carried out; (4) the catalyst was scraped out and made into the KBr pellet. R_1, R_2 and R_3 represent the photooxidation rates of first, second and third run, respectively. Fig. 9 shows the R_1, R_2 and R_3 of the seven regeneration processes. Fresh catalyst was used at the first time so that the R_1 of every process was about 0.19 μmol cm^{-2} min^{-1}. The recovery of catalyst activity was obviously variable after different regeneration processes. The oxidation efficiency after the regeneration processes followed the sequence: H_2O_2/UV ≅ H_2O_2 > H_2O/UV > WA/UV > O_2/UV > DA/UV > DA.

Oxygen plays an important role in the photocatalytic oxidation. The recovery of catalyst activity of the O_2/UV processes was better than the DA/UV one. In O_2/UV process, increasing the content of oxygen increased the production of super-oxide anion radicals (Eq. (11)). The more amount of $^{\bullet}O_2^-$ could oxidize the intermediates adsorbed on TiO_2 surface in these processes.

Water can trap the holes to form hydroxyl radicals (Eq. (10)). The WA/UV process could produce more hydroxyl radicals than DA/UV process. Hydroxyl radicals are stronger than super-oxide anion radicals. Hence, the WA/UV process was more effective to recover the activity of catalyst than DA/UV and O_2/UV processes. Obviously, the gas regeneration processes (WA/UV, O_2/UV, DA/UV, DA) did not recover the activity of catalyst completely. The direct surface treatment was adopted to regenerate the catalyst activity. Water and hydrogen peroxide were used to clean the catalyst surface. The catalyst activity was almost recovered by H_2O_2/UV, H_2O_2, H_2O/UV processes.

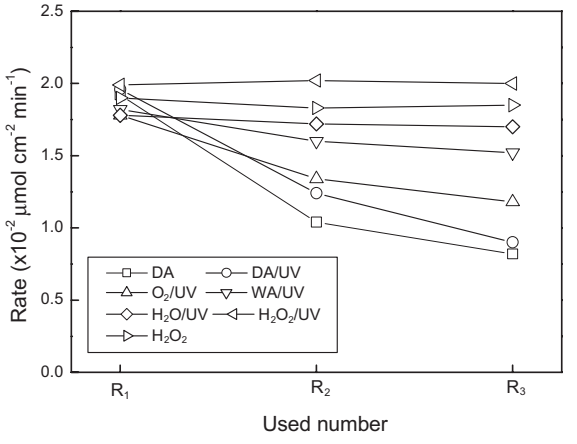

Fig. 9. The variation of DMF conversion in different regeneration processes. (Experimental condition: inlet DMF concentration = 25.1 μM; oxygen content = 20%; humidity = 3.25 μM; reaction temperature = 100 °C; area of catalyst film = 170 cm^2.)

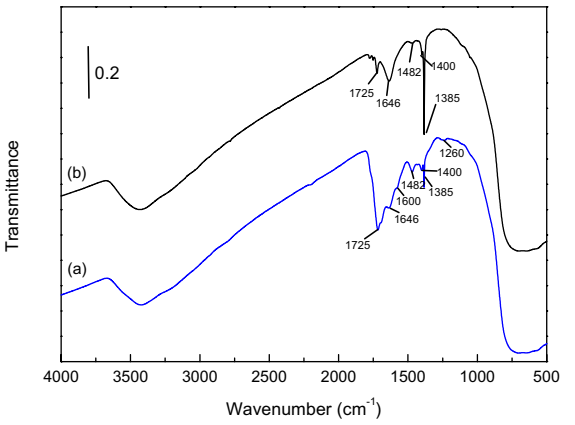

Fig. 10. FTIR spectra of catalyst after (a) DA process and (b) H_2O_2/UV process.

The FTIR spectra of TiO_2 surface after DA process and H_2O_2/UV process are shown in Fig. 10. The spectrum after DA process (Fig. 10(a)) is similar to the one after DMF oxidation 150 min (Fig. 8(c)). It also displays that most adsorbed species on catalyst surface were not taken away by the dry air. These species might be formaldehyde, formic acid and methylamine. They chemisorbed on the catalyst surface and caused the catalyst deactivation. Many vibration peaks of organic function groups decreased after H_2O_2/UV process. The C=O stretch at 1725 cm^{-1} decreased indicating the degradation of formaldehyde and formic acid. The intensity of the band at 1600 cm^{-1} decreased while the N–O stretching vibration of NO_3^- at 1385 cm^{-1} increased. It indicates that methylamine had been oxidized to form NO_3^-.

4. Conclusions

Titanium dioxide thin film coated on glass was an active catalyst for the photooxidation of DMF. The oxidation rate was found to be dependent on inlet concentration of DMF, reaction temperature, water vapor, and oxygen content. The reaction rate was faster at higher inlet concentration. Increasing reaction temperature for the DMF oxidation increased the reaction rate

when the temperature was under 150 °C. The water vapor enhanced the degradation of DMF at low humidity but inhibited the reaction at high water content. When the oxygen content was higher than 20%, the conversion rate was almost kept at constant. The deactivation of catalyst was observed in the photooxidation of DMF. The kinetics of deactivation can be described by the Levenspiel deactivation kinetic model. Catalyst deactivation was more significant at lower reaction temperature and oxygen content. Carboxylic acids, aldehydes, nitrogen-containing intermediates, ammonium, nitrate and carbonate were present on the surface of used catalyst. The intermediates of DMF photooxidation may be formaldehyde, formic acid and methylamine. These intermediates and final products deactivated the catalyst by blocking active sites. Four gas treatment processes and three liquid treatment processes were used to recover the activity of catalyst. The liquid treatment processes were more effective than the gas treatment ones, because these species on used catalyst surface were oxidized by H_2O_2/UV regeneration process. Additionally, the amount of nitrate on catalyst surface increased after regeneration process, indicating that the oxidation of nitrogen-containing intermediates happened due to the regeneration processes.

Acknowledgments

This work has been supported by National Science Council, Taiwan, ROC (Grant NSC92-2211-E009-028).

References

Alberici, R.M., Canela, M.C., Eberlin, M.N., Jardim, W.F., 2001. Catalyst deactivation in the gas phase destruction of nitrogen-containing organic compounds using TiO_2/UV–VIS. Appl. Catal. B: Environ. 30, 389–397.

Brinkley, D., Engel, T., 1998. Photocatalytic dehydrogenation of 2-propanol on TiO_2(1 1 0). J. Phys. Chem. B 102, 7596–7605.

CDCP (Centers for Disease Control and Prevention), 1989. Testicular cancer in leather workers—Fulton County, New York. MMWR 38, 105–114.

Ducatman, A.M., Conwill, D.E., Crawl, J., 1986. Germ-cell tumors of the testicle among aircraft repairman. J. Urol. 136, 834–836.

Huang, A., Coa, L., Chen, J., Spiess, F.-C., Suib, S.L., Obee, T.N., 1999. Photocatalytic degradation of triethylamine on titanium oxide thin films. J. Catal. 188, 40–47.

Kim, S.B., Hwang, H.T., Hong, S.C., 2002. Photocatalytic degradation of volatile organic compounds at the gas–solid interface of TiO_2 photocatalyst. Chemosphere 48, 437–444.

Klare, M., Scheen, J., Vogelsang, K., Jacobs, H., Broekaert, J.A.C., 2000. Degradation of short-chain alkyl- and alkanolamines by TiO_2- and Pt/TiO_2-assisted photocatalysis. Chemosphere 41, 353–362.

Levenspiel, O., 1999. Deactivation catalyst. In: Chemical Reaction Engineering, third ed. Wiley, pp. 473–478.

Lin, S.S., Wu, C.S., Cheng, H.T., 1999. The best available control technology for gaseous emission of DMA from factories of polyurethane synthetic leather. In: Proceedings of the 16th Air Pollution Control Technology Conference, Taiwan, pp. 261–264.

Linsebigler, A.L., Lu, G., Yates, J.T., 1995. Photocatalysis on TiO_2 surfaces: principles, mechanisms, and selected results. Chem. Rev. 95, 735–758.

Monzón, A., Romeo, E., Borgna, A., 2003. Relationship between the kinetic parameters of different catalyst deactivation models. Chem. Eng. J. 94, 19–28.

Niu, F., Hofmann, H., 1997. Studies on deactivation kinetics of a heterogeneous catalyst using a concentration-controlled recycle reactor under supercritical conditions. Appl. Catal. A 158, 273–285.

Peral, J., Ollis, D.F., 1992. Heterogeneous photocatalytic oxidation of gas-phase organics for air purification: acetone, 1-butanol, butyraldehyde, formaldehyde, and *m*-xylene oxidation. J. Catal. 136, 554–565.

Peral, J., Ollis, D.F., 1997. TiO_2 photocatalyst deactivation by gas-phase oxidation of heteroatom organics. J. Mol. Catal. A 115, 347–354.

Piera, E., Ayllón, J.A., Doménech, X., Peral, J., 2002. TiO_2 deactivation during gas-phase photocatalytic oxidation of ethanol. Catal. Today 76, 259–270.

Sauer, M.L., Ollis, D.F., 1996. Catalyst deactivation in gas-solid photocatalysis. J. Catal. 163, 215–217.

Snell, F.D., Snell, C.T., 1949. Colorimetric Methods of Analysis, vol. II, third ed. D. Van Nostrand Company, New York.

Sun, R.-D., Nakajima, A., Watanabe, T., Hashimoto, K., 2003. Decomposition of gas-phase octamethyltrisiloxane on TiO_2 thin film photocatalysts—catalytic activity, deactivation, and regeneration. J. Photochem. Photobiol. A 154, 203–209.

WHO, IARC, 1989. IARC monographs on the evaluation of carcinogenic risk to humans. Some organic solvents, resin monomers and related compounds, pigments and occupational exposures in paint manufacture and painting, vol. 47. IARC, Lyon, France.

Xu, W., Raftery, D., 2001. Photocatalytic oxidation of 2-propanol on TiO_2 powder and TiO_2 monolayer catalysts studies by solid-state NMR. J. Phys. Chem. B 105, 4343–4349.

Yamazaki, S., Tanaka, S., Tsukamoto, H.S., 1999. Kinetic studies of oxidation of ethylene over a TiO_2 photocatalyst. J. Photochem. Photobiol. A 121, 55–61.

Zhao, J., Yang, X., 2003. Photocatalytic oxidation for indoor air purification: a literature review. Build. Environ. 38, 645–654.